International Conference on Control, Engineering & Information Technology (CEIT'13)
Proceedings Engineering & Technology - Vol.1, pp. 186-191, 2013

Rotor Fault Diagnosis in Three Phase Induction Motors Using the Wavelet Transform

Ahcène Bouzida[#1], Omar Touhami[#1], Radia Abdelli[*2]

[#] *Ecole Nationale Polytechnique, Algiers*
Algiers 16200, Algérie
[1]bouzida.umbb@gmail.com

[*]*Electrical Engineering Departement Abderrahmane MIRA(BEJAIA) University*
TARGA OUZEMOUR (TAGHZOUIT) Béjaia -6000-Algérie
[2]abdelli_radia@yahoo.fr

***Abstract*— In this paper the faults diagnosis of induction machines based on the discrete wavelet transform (DWT) is detailed. The wavelet decomposition is used to extract the information from a signal over a wide range of frequencies. This analysis is performed in both time and frequency domains. The Daubechies wavelet is selected for the analysis of the stator current. Wavelet components appear to be useful for detecting different electrical faults. In this paper we will study the problem of broken rotor bars, and end-ring segment.**

***Keywords*— Fault diagnosis, Induction Machines, broken end-ring, broken rotor bars, Wavelet transform, Decomposition level**

I. Introduction

The induction machines were dedicated for electric drives and play an important role in manufacturing environments. Therefore this type of machines is generally considered and several diagnostic procedures are proposed in the literature [l]–[10].

Specific uses of induction machines do not tolerate inopportune breakdowns. These breakdowns can be due to the machine and can be of mechanical origin (rotor eccentricity, coupling defect, bearings defects, etc…) or electric and magnetic origin (short circuit in stator windings, broken bars, broken end-ring or broken teeth).

Wavelet transform is an analysis method for time varying or non-stationary signals, and uses a description of spectral decomposition via the scaling concept. Wavelet theory provides a unified framework for a number of techniques which have been developed for various signal processing applications [10]–[18]. One of its feature is multi-resolution signal analysis with a vigorous function of both time and frequency localization. This method is effective for stationary signal processing as well as non-stationary signal processing. References [19],[20] describe the pyramidal algorithm based on convolutions with quadrature mirror filters which is a fast method similar to FFT (Fast Fourier Transform) for signal decomposition and reconstruction. It can be interpreted as a decomposition of the original signal in an orthonormal wavelet basis or as a decomposition of the signal in a set of independent frequency bands. This independence is due to the orthogonality of the wavelet functions [21].

In this paper, a method for the diagnosis of broken rotor bars and broken end is described. Several experiments are developed for different fault cases and operating conditions such as healthy rotor, one broken bar, two broken bars, and one end-ring portion broken. The experiments have been especially done at the laboratory on four constructed machines for diagnosis purposes.

II. Description of The Wavelet Method

The wavelet method requires the use of time-frequency basis functions with different time supports to analyze signal structures of different sizes. The wavelet transform, an extension of the Short-time Fourier Transform, projects the original signal down onto wavelet basis functions and provides a mapping from the time domain to the time-scale plane.

A wavelet is a function belonging to $L^2(R)$ with a zero average. It is normalized and centered on the neighborhood of $t = 0$. A time-frequency atom family is obtained by scaling a band pass filter ψ by s and translating it by u.

L2(R) represents the space vector of measurable square-integrable functions on the real line R with $\|\psi\| = 1$.

$$\int_{-\infty}^{+\infty} \psi(t)\, dt = 0 \tag{1}$$

$$\psi_{u,s}(t) = \frac{1}{\sqrt{s}} \psi\left(\frac{t-u}{s}\right) \tag{2}$$

The wavelet transform of a function f at the scale s and position u is computed by correlating f with a wavelet atom:

$$W_f(u,s) = \int_{-\infty}^{+\infty} f(t) \frac{1}{\sqrt{s}} \psi.\left(\frac{t-u}{s}\right) dt \tag{3}$$

A real wavelet transform is complete and conserves energy as long as it satisfies a weak admissibility condition:

$$\int_{0}^{+\infty} \frac{|\psi(\omega)|^2}{|\omega|} d\omega = \int_{-\infty}^{0} \frac{|\psi(\omega)|^2}{|\omega|} d\omega = C_\psi < +\infty \tag{4}$$

When *Wf(u,s)* is known only for $s<s0$, we need to recover *f*, a complement of information corresponding to *Wf (u,s)* for $s>s0$. This is obtained by introducing a scaling function φ that is a wavelets aggregate at scales larger than

1. In the sequel, we design by $\hat{\psi}(\omega)$ and $\hat{\varphi}(\omega)$ the Fourier transforms of $\psi(n)$ and $\varphi(n)$, respectively.

When $W_f(u, s)$ is known only for $s<s_0$, we need to recover f, a complement of information corresponding to $W_f(u, s)$ for $s>s_0$. This is obtained by introducing a scaling function φ that is a wavelets aggregate at scales larger than 1. In the sequel, we design by $\hat{\psi}(\omega)$ and $\hat{\varphi}(\omega)$ the Fourier transforms of $\psi(n)$ and $\varphi(n)$, respectively.

The discrete wavelets transform results from the continuous version. Unlike this latter, the DWT uses a discrete scale factor and a translation. One calls discrete wavelet transform dyadic into any base of wavelet working with a scale factor $u = 2^j$.

The discrete version of Wavelet Transform, DWT, consists of sampling neither the signal nor the transform but sampling the scaling and shifted parameters, [25-27]. This results in high frequency resolution at low frequencies and high time resolution at high frequencies, removing the redundant information. Taking positive frequency into account, $\hat{\varphi}(\omega)$ has information in $[0, \pi]$ and $\hat{\psi}(\omega)$ in $[\pi, 2\pi]$. Therefore they both have complete signal information without any redundancy. Functions $h(n)$ and $g(n)$ can be obtained by inner product of $\psi(t)$ and $\varphi(t)$. Decomposition of the signal in $[0, \pi]$ gives [10]:

$$h(n) = < 2^{-l}\varphi(2^{-l}t)\varphi(t-n) >$$
$$g(n) = < 2^{-j}\psi(2^{-j}t)\varphi(t-n) >,\ j = 0,1,\ldots, \quad (5)$$

Wavelet decomposition does not involve the signal in $[\pi, 2\pi]$. In order to decompose the signal in the whole frequency band, wavelet packets can be used. After decomposing l times, we get 2^l frequency bands each with the same bandwidth that is:

$$\left[\frac{(i-1)f_n}{2},\ \frac{if_n}{n}\right] \qquad i = 1,\ 2,\ \ldots,2^l \quad (6)$$

where fn is the Nyquist frequency, in the i^{th}-frequency band. Wavelet packets decompose the signal into one low-pass filter $h(n)$ and $(2^l - 1)$ band-pass filters $g(n)$, and provide diagnosis information in 2 frequency bands. A_i is the low frequency approximation and D_i is the high frequency detail signal, both at the resolution j:

$$A_j(n) = \sum_k h(k-2n)A_{j-1}$$
$$D_j(n) = \sum_k g(k-2n)A_{j-1} \qquad n = 1,2,3\ldots\ldots \quad (7)$$

where $A_0(k)$ is the original signal. After decomposing the signal, we obtain one approximation signal A_i and D_i detail signals (see Fig.1).

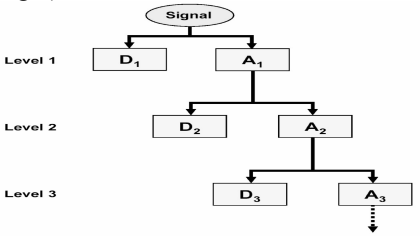

Fig.1. Tree decomposition of the signal S

The wavelet packets method is a generalization of wavelet decomposition that offers a richer range of possibilities for signal analysis (see Fig.2). In wavelet analysis, a signal is split into an approximation and a detail. Then the approximation is itself split into a second-level approximation and detail, and the process is repeated [23] till the targeted results are obtained. For n-level decomposition, there are $n+1$ possible ways to decompose or encode the signal:

$$W_{2n}(t) = \sqrt{2}\sum_k h(k)W_n(2t-k)$$
$$W_{2n+1}(t) = \sqrt{2}\sum_k g(k)W_n(2t-k) \quad (8)$$

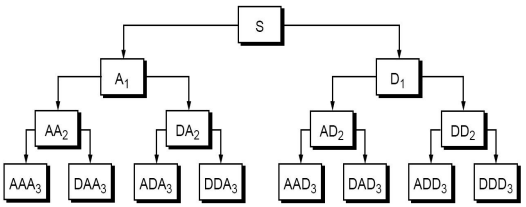

Fig.2 Decomposition of the signal S in wavelet packet

where $W(t)$ *is* the original signal. By comparing Eqs. (8) With Eqs. (7), we can find that only A_j in Eq. (7) is decomposed but also D_i in Eq.(8) is decomposed.

Wavelets and wavelet packets decompose the original signal which is non-stationary or stationary into independent frequency bands with multi-resolution [23].

III. Experimental Tests

A. Motor Current Signature Analysis

Four rotors have been used in the tests as shown in Fig. (3). In order to obtain correct resolution for the wavelet analysis, it is important to choose correctly the acquisition parameters, i.e. the sampling frequency and number of samples. Some constraints are also taken into consideration:

- Analyzed signal bandwidth,
- Wavelet decomposition spectral bands,
- Frequency resolution,
- Appropriate number of decomposition.

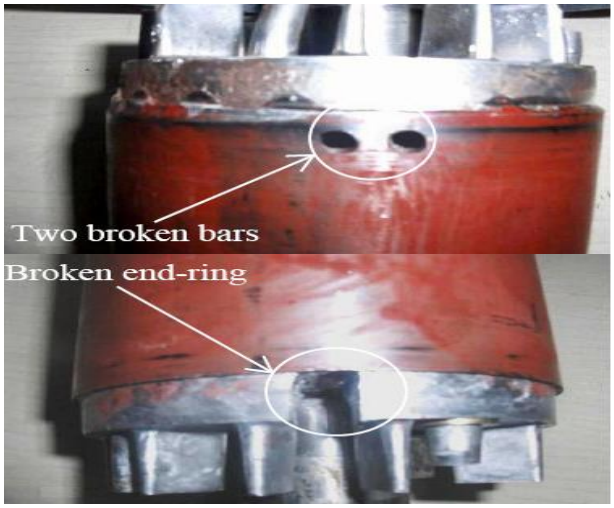

Fig.3. Faulty rotors under tests

For an induction machine, the significant information in stator current signal is concentrated the *0-400 Hz* band. Applying the Shannon's theorem, yields minimum sampling frequency *fs* of *800Hz*.

The minimum resolution needed to get a good result is 0.5 Hz. Eq. (9) defines the number of samples, N_s, needed for a given resolution *R*, [19]–[21].

$$N_S = \frac{f_S}{R} \tag{9}$$

In our case, we have chosen a sampling frequency *fs* =10 *kHz* to obtain a good frequency resolution. Hence, N_s *=100000* samples are acquired for *R=0.1Hz*. The analyzing frequencies vary from 0 to *5 kHz* with a resolution of *0.1Hz*.

Fig.4 shows the experimental setup where different 4kW induction machines are used to test the performance of the proposed methodology identifying different faults treated in this work. This system can be used to sample two line currents *Ia* and *Ib*, three line voltages V_a , V_b *and* V_c , and a speed signal. The stator windings are star connected. The main parts of the experimental setup are as follows:

Fig.4: Experimental setup

- Three-phase 4-kW induction machine,
- DC generator coupled to the IM to provide load,
- PC equipped with a data acquisition (IOTEQ DAQ2000 SERIES) card.

The tested machines have two pole-pairs (p=2), 28 bars and receive a power supply of 220V AC at 50Hz. For the rotor faults the machines are tested at 75% of rated load and no load for the loss of stator phase test.

We have experimented a method for the selection of wavelet decomposition level namely the approach presented in [25], the approach is based on the sampling frequency.

B. Selection of the decomposition level

The approach is based on:

- A suitable number of decomposition levels (n_{Ls}) depend on the sampling frequency *fs* of the signal being analyzed. For each one of the proposed approaches [22],[24],[25] it has to be chosen in order to allow the high-level signals (approximation and details) to cover all the range of frequencies along which the sideband is localized.
- The minimum number of decomposition levels that is necessary for obtaining an approximation signal (A_{nf}) so that the upper limit of its associated frequency band is under the fundamental frequency [16], is described by the following condition:

$$2^{-(n_{Ls}+1)} f_s < f \tag{12}$$

From this condition, the decomposition level of the approximation signal which includes the left sideband harmonic is the integer n_{Ls} given by:

$$n_{Ls} = int(\frac{log(fs/f)}{log(2)}) \tag{13}$$

For this approach, further decomposition of this signal has to be done so that the frequency band *[0–f]* will be decomposed in more bands. Usually, two additional decomposition levels (that is, n_{Ls} +2) would be adequate for the analysis [16].

$$n_{Ls} + 2 = int(\frac{log(10000/50)}{log(2)}) + 2 \tag{14}$$
$$= int(7.64) + 2 = 9\,levels$$

For this case the wavelet decomposition tree is showed in Table II.

TABLE I
FEQUENCY BANDS OBTAINED BY DECOMPOSITION IN MULTILEVELS

Level	**Approximations**		**Details**	
J = 1	A1	0 - 5000	D1	5000 - 10000
J = 2	A2	0 - 2500	D2	2500 - 5000
J = 3	A3	0 - 1250	D3	1250 - 2500
J = 4	A4	0 – 625	D4	625 - 1250
J = 5	A5	0 - 312.50	D5	312.5 - 625
J = 6	A6	0 - 156.25	D6	156.25 - 312.5
J = 7	A7	0 - 78.125	D7	78.125 - 156.25
J = 8	A8	0 -39.0625	D8	39.0625 - 78.125
J = 9	A9	0 - 19.5313	D9	19.53 - 39.0625

Several types of mother wavelets exist (Daubechies, coiflet, simlet, biorthogonal, etc…..) and have different properties,

[17]. However, some authors showed that all these types of mother wavelets gave similar results. Due to the well-known properties of the orthogonal Daubechies family, we chose to use a mother wavelet of this family.

The multilevel decomposition of the stator current was then performed using Daubechies wavelet, the suitable level of decomposition is calculated according to Eq. (13). When the defect of the rotor bars, end-ring portion, and short-circuit on the stator windings of the induction motor appear, the defect information in stator current is included in each frequency band determined by the decomposition in wavelet or in wavelet packet. By calculating the energy associated to each level or with the each node of decomposition, one can build a very effective diagnosis tool. The energy eigenvalue for each frequency band is defined by [19]-[21]:

$$E_j = \sum_{k=1}^{k=n} \left| D_{j,k}(n) \right|^2 \quad (15)$$

Based on the energy eigenvalue, the eigenvector is set up as:

$$T = \left[\frac{E_0}{E}, \frac{E_1}{E}, \frac{E_2}{E}, ..., \frac{E_{2^l-1}}{E} \right] \quad (16)$$

where j=*1,2...,*2^l*-1*; D_j is the amplitude in each discrete point of the wavelet coefficient of the signal in the corresponding frequency band, with $E = \sum_{j=0}^{2^m-1} \left| E_j \right|^2$

The eigenvalue T contains information on the signal of the stator current for a motor behavior. Besides, the amplitudes of the deviation of some eigenvalues indicate the severity of the defect, which makes T a good candidate to diagnose broken bars of the rotor and/or defect of the end-ring portion.

The PSD of the stator current clearly shows the increase of the amplitudes in relation with the defects of the rotor (1±2s)f. Fig (5 and 6) show the PSD of the stator current in the cases of healthy machine and machine with two broken bars.

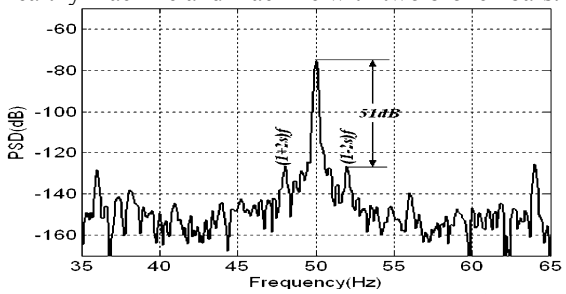

Fig.5. Normalized PSD of the stator current of a healthy induction machine

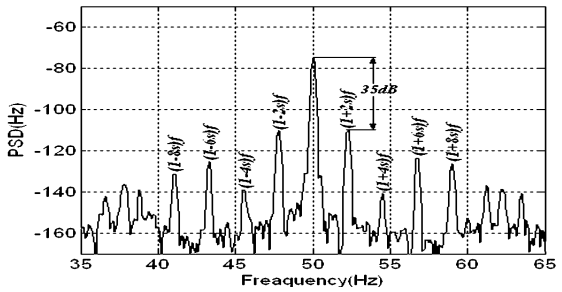

Fig.6. Normalized PSD of the stator current of an induction machine with two broken rotor bars

C. *Discrete Wavelet Transform Applied to the Stator Current*

The "Daubechies wavelets" of different order are used to decompose the stator current of each machine. Fig(9) represents the detail and approximation signals (*D9, D8, D7* and *A6*) obtained by *db44*. The calculation of the energy eigenvector T indicates the variation of this energy in the four machines as shown in Figs. (8, 9 and 10)

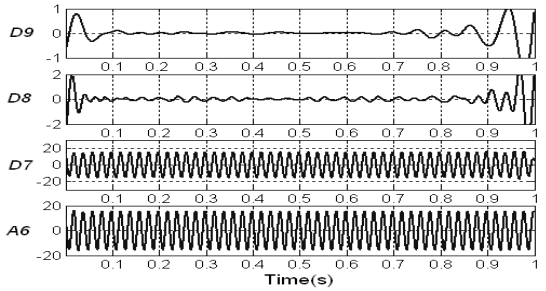

(a)

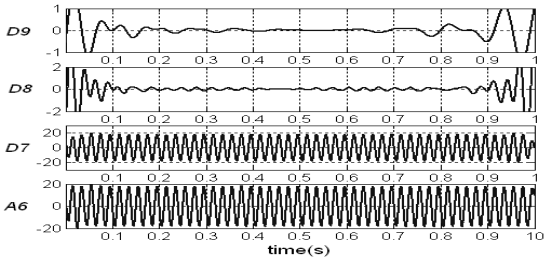

(b)

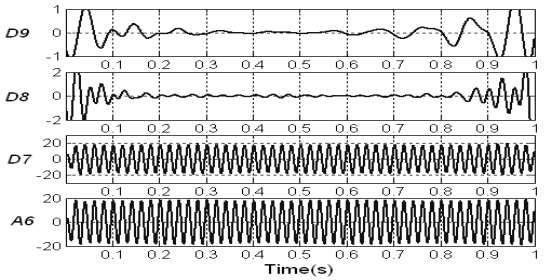

(c)

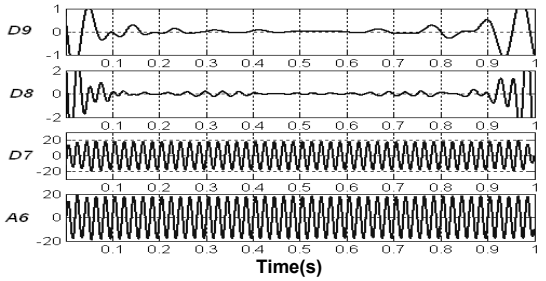

(d)

Fig.7. Details and approximation for a) healthy, b) one broken bar, c) two broken bars and d) broken end-ring

In Fig.7, the evolution in the observed frequency bands of the relative signal to the rotor defect can be analyzed using coefficients D9 and *D8* to *D7* or using only coefficient *A6* that gives all the information in the frequency band [*0-156.25Hz*]. While analyzing the effect of the rotor defect in the bands of

interesting frequencies, one shows that the energy depends on the type of defect. For all the studied machines, the difference between the healthy rotor and the deficient rotors is clearly shown in Fig. 7.

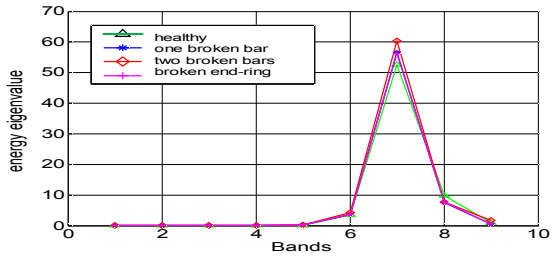

Fig.8. Eigenvector analysis results obtained from db6

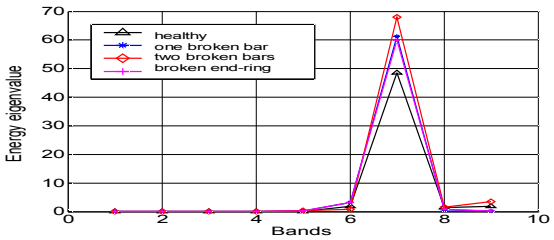

Fig.9. Eigenvector analysis obtained from db24

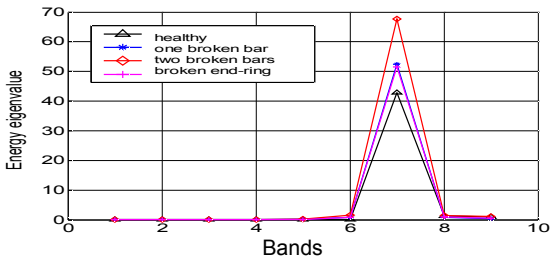

Fig.10. Eigenvector analysis results obtained from db44

Fig (9 and 10) clearly show the variation of the energy eigenvalue. One can observe that the energy stored in band 7 depends on the degree of the default. Obviously, the energy in level 7 represents the number of broken bars and the broken end-ring portion of the squirrel cage rotor. Fig (8, 9 and 10) show that the choice of the mother wavelet and its order has a great importance in differentiating the energies, because when the order of the mother wavelet is increased the difference between the energy eigenvalues becomes clearer.

The band of detection of broken rotor bars can't be influenced by mechanical vibrations and load effect because the frequencies accompanying the mechanical problem are very far from the band of detection which is located in [39.06-78.12]Hz. The broken bar and end-ring portion induce supplementary frequencies near the fundamental component which are described by *(1±2s)f*. These frequencies are influenced only by the operating frequency *f* and the slip *s,* however this method is not dependent on the motor power, but we must choose the appropriate band and the decomposition of the stator current.

D. Application to Residual Stator Current

The extraction of the fundamental component leads to a signal full of in information. Indeed the elimination of the dominant component in the stator current contributes to amplify the components due to defects. For this reason we make the stator current go through a band-pass filter to elimination the 50Hz frequency. This method produces attenuation in some components.

Fig (11 and 12) represent the variation of the energy eigenvalue.

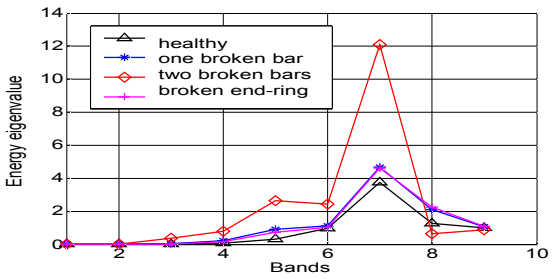

Fig.11. Eigenvector analysis results obtained from db24

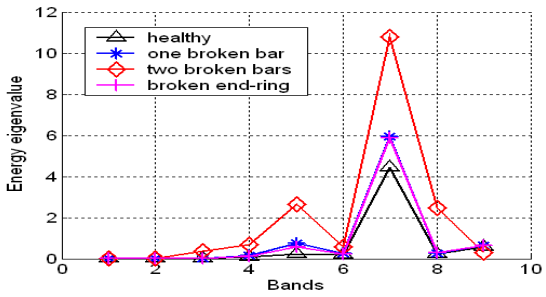

Fig.12. Eigenvector analysis results obtained from db6

Looking at Fig (11) and (12), one can note that the extraction of the fundamental has a very significant effect on the diagnosis of defaults. This effect is interpreted by the increase in the amplitudes of the signals in bands D7 and A6, in the case of defect compared to the healthy case. The effect of the extraction also led to a differentiation in the energies stored in the levels between the various machines not only in level 7 but in levels 1, 2, 3, 4, 5, 6 as well 7. According to the previous results, one can also note that the effect of the broken rotor bar is similar to that of a broken end-ring portion.

IV. CONCLUSION

Signal decomposition via wavelet transform and wavelet packets provides a good approach of multi-resolution analysis. The decomposed signals are independent due to the orthogonality of the wavelet function. There is no redundant information in the decomposed frequency bands.

Based on the information from a set of independent frequency bands, mechanical condition monitoring and fault diagnosis can be effectively performed.

This work shows a new approach in detection of broken rotor bars in induction motor having only stator currents as input. The detection is based on the Discrete Wavelet

Decomposition method. The results show the effectiveness of the proposed method for this kind of fault.

MCSA is a good method for analyzing motor faults over constant load torque. But in the case of non constant load torque or non-stationary signals, the use of the wavelet decomposition is required.

REFERENCES

[1] M. E. H. Benbouzid "A review of induction motors signature analysis as a medium for faults detection," IEEE Trans. On Industrial Electronics, vol. 47, pp. 984–993, Oct. 2000.

[2] M. E. H. Benbouzid, M. Vieira, C. Theys. "Induction Motors Faults Detection and Localisation Using Stator Current Advanced Signal Processing Techniques, IEEE, " Transaction on Power Electronics, Vol 14 n°1, pp 14-22, Jan 1999.

[3] S. A. Al Kazzaz Sa'ad, G.K.Singh, "Experimental investigations on induction machine condition monitor and fault diagnosis using digital signal processing techniques, " Electric Power Systems Research 65, pp 179-221, 2003.

[4] Hua Su, Kil To Chong, "Induction Machine Condition Monitoring Using Neural Network Modeling," IEEE Trans. on Industrial Electronics, vol. 54, No. 1, pp. 241-249, Feb 2007.

[5] A. Lebaroud, G. Clerc, "Classification of induction machine faults by optimal time–frequency representations," IEEE Trans. On Industrial Electronics, vol. 55, pp. 4290-4298, Dec. 2008.

[6] Pineda-Sanchez M., Riera-Guasp M., José A. Antonio-Daviu, J. Roger-Folch, J. Perez-Cruz and R. Puche-Pandero. Diagnosis of induction motor faults in the fractional Fourier domain. IEEE Transaction on Instrumentation and Measurement, Digital object Identifier 10.1109/TIM.2009.2031835, 2009.

[7] B. Akin, U. Orguner, H.A. Toliyat, M. Rayner, "Low Order PWM Inverter Harmonics Contributions to the Inverter-Fed Induction Machine Fault Diagnosis," IEEE Transaction on Industrial Electronics, vol. 55, no. 2, pp. 610-619, Feb 2008

[8] J. F. Martins, V. Ferno Pires, A. J. Pires, "Unsupervised Neural-Network-Based Algorithm for an On-Line Diagnosis of Three-Phase Induction Motor Stator Fault," Trans. on Industrial Electronics, vol. 54, No. 1, pp. 259-264, Feb 2007.

[9] M. E. H. Benbouzid, G. B. Kliman, "What Stator Current Processing Based Technique to Use for Induction Motor Rotor Faults Diagnosis?," IEEE, Transaction on Energy Conversion, Vol. 18, N°2, pp 238-244, June 2003.

[10] T. Tarasiuk, "Hybrid wavelet–Fourier spectrum analysis," IEEE Trans. Power Del., vol. 19, No. 3, pp. 957–964, Jul. 2004.

[11] Jose A. Antonio-Daviu, Martin Riera-Guasp, José Roger Floch, and M. Pilar Molina Palomares, Validation of a new method for the diagnosis of rotor bar failures via wavelet transform in industrial induction machines, "IEEE Trans. On Ind. Appl., vol.42, N°4, pp.990 – 996, July/August 2006

[12] Faiz, J.; Ebrahimi, B.M.; Asaie, B.; Rajabioun, R.; Toliyat, H.A. " A criterion function for broken Bar fault diagnosis in Induction Motor under load variation using Wavelet Transform, " ICEMS International Conference on Electrical Machines and Systems, pp.1249-1254, 2007.

[13] M. A. S. K. Khan, Tawkik S. Radwan, and M. Azizur Rahman. Real-time implementation of wavelet packet transform-based diagnosis and protection of three-phase induction motors. IEEE Trans. On Energy Conversion, vol.22, n°3, pp.647-655, Sept.2007

[14] J. Cusidó, L. Romeral, J. A. Ortega, J. A. Rosero, A. G. Espinosa, "Fault detection in induction machines using power spectral density in wavelet decomposition," IEEE Trans. On Ind. Electron., vol. 55, pp. 633-643, Feb. 2008.

[15] A. Ordaz-Moreno, R. de J. Romero-Troncoso, J. A. Vite-Frias, J. R. Rivera-Gillen, A. Garcia-Perez, "Automatic online diagnosis algorithm for broken-bar detection on induction motors based on discrete wavelet transform for FPGA implementation," IEEE Trans. On Ind. Electron., vol. 55 , pp. 2193-2202, May. 2008.

[16] J. A. Daviu, M. Riera-Guasp, J. Roger-Folch, F. Martínez-Giménez, A. Peris, " Application and Optimization of the Discrete Wavelet Transform for the Detection of Broken Rotor Bars in Induction Machines, " Applied and Computational Harmonics Analysis, pp 268–279, 2006.

[17] J.K. Zhang, T.N. Davidson, K.M. Wong, Efficient design of orthonormal wavelet bases for signal representation, IEEE Trans. Signal Process., vol.52, N°7, pp. 1983–1996, 2004.

[18] Shahin Hedayati Kia, Humberto Henao, and Gérard-André Capolino. Diagnosis of broken-bar fault in induction machines using discrete wavelet transform without slip estimation. IEEE Trans. Ind. Applications., vol. 45, n°4, pp. 1395 - 1404, July/August 2009.

[19] Cvetkovic, Z., and Vetterli, M.: 'Discrete-time wavelet extrema representation: design and consistent reconstruction', IEEE Trans. Signal Process., N°3, pp. 681–693, 1995.

[20] Faliang Niu; Jin, Huang; "Rotor broken bars fault diagnosis for induction machines based on the wavelets ridge energy spectrum" ICEMS Eight International Conference on Electrical Machines and Systems,vol.3, pp.2274-2277, 2005.

[21] Tommy W. S. Chow and Shi Hai, "Induction machine fault diagnostic analysis with wavelet technique" IEEE Trans. on Industrial Electronics, vol.51, N°3, pp 558-565, June 2004.

[22] O.A. Mohamed, N.Y. Abed and S.C. Ganu. Modelling and Characterization of induction motor internal faults using Finite element and discrete wavelet transform. IEEE Transaction On Magnetics, vol.42, pp.3434-3436, 2006

[23] S. Rajagopalan, J.M. Aller, J.A. Restrepo, T.G. Habetler, R.G. Harley, "Analytic-Wavelet-Ridge-Based Detection of Dynamic Eccentricity in Brushless Direct Current (BLDC) Motors Functioning Under Dynamic Operating Conditions," IEEE Transaction on Industrial Electronics, vol. 54, no. 3, pp. 1410-1419, June 2007.

[24] Supangat, R.; Ertugrul, N.; Soong, W.L.; Gray, D.A.; Hansen, C.; Grieger, J., " Detection of broken rotor bars in Induction Motor using Starting-current Analysis and Effects of Loading" IEE Proceedings Electric Power Applications, vol.153, n°6, pp.848-855, 2006.

[25] Zhongming Ye, Bin Wu, A. Sadeghian, "Current signature analysis of induction motor mechanical faults by wavelet packet decomposition," IEEE Trans. on Industrial Electronics, vol. 50, no. 6, pp. 1217- 1228, Dec 2003.

[26] P. Rodriguez. "Current-, Force- and Vibration based Techniques for Induction Motor Condition Monitoring, PhD Thesis, Helsinki University of Technology, 2007.

[27] T. K. Sarkar, M. Salazar-Palma, and M. C. Wicks, Wavelet Applications in Engineering Electromagnetics. Norwood, MA: Artech House, 2002.

[28] MV Mickerhauser, Adapted Wavelet Analysis from Theory to Software. Natick, MA: Wellesley, 1994

[29] A.N. Akansu, R. A. Haddad, Multi-resolution Signal Decomposition Transforms, Sub-bands, and Wavelets, Second Edition, New Jersey Institute of Technology Newark, NJ, ACADEMIC PRESS, 2001.

[30] M. Misiti Y. Misiti G. Oppenheim J. M. Poggi, Wavelet Toolbox, User's Guide for Matlab, Version 2.1, MATHWORKS.

[31] J. Cusido, A. Jornet, L. Romeral, J.A. Ortega, A.Garcia, "Wavelet and PSD as a Fault Detection Techniques, " IEEE - IMTC Instrumentation and Measurement, pp1397-1400, 2006